



Synergetic Effect of Cement Kiln Flue Dust for Enhancing Physicomechanical Properties of Metakaolin-Blended Cement



CrossMark

Mohamed G. Ismail,^a Mahmoud Gharieb,^{b,*} Mohamed E. Sultan,^a Hamdy A. Hammad^a

^aChemistry Department, Faculty of Science, Al-Azhar University, Nasr City, P.B. 11884, Cairo, Egypt

^bRaw Building Materials Technology and Processing Research Institute, Housing & Building National Research Centre (HBRC), Cairo, Egypt

Abstract

As a result of the increasing impact of cement kiln flue dust on human health and the environment. In this study, cement kiln flue dust was used as an alkaline activator for mixed cement made from ordinary Portland cement (OPC) and metakaolin (MK). In the first part of the research, the different proportions of cement and metakaolin were studied to obtain the best-blended mixes. Various ratios of metakaolin were substituted for MK (5, 10, 15, 20, and 25 %) to obtain the best ratio between OPC and MK. Incorporation of cement kiln flue dust in 15MK mix by different weight ratios (2, 4, 6, 8, and 10%) as a partial substitution ratio from OPC ratio was investigated to improve the pozzolanic activity of MK, especially at early ages of hydration. To realize and investigate the effect of cement kiln flue dust on MK cement binder, classical tests of setting times and strength at various ages. The results were analyzed by using advanced devices. The results indicated that the MK has a positive effect on the physicomechanical properties of cement. The 15MK mix exhibited the best results regarding the physicochemical of hardened cement paste, especially at later ages of hydration. The compressive strength of the 15MK mix increased by about 23.53% compared with the neat OPC at 28 days of hydration. Based on the physicochemical and mechanical measurement, the incorporation of 6% CKFD with 15 % MK in blended cement paste improved the physico-mechanical properties of the hardened cement by the formation of calcium silicate hydrate and reduces Ca (OH)₂ to lower limits and reduces the waste results from the cement industry.

Keywords: Blended Cement; Cement Kiln Flue Dust (CKFD); microstructure; metakaolin; Setting time; compressive strength

1. Introduction

Global warming, which is closely tied to the Greenhouse Gas (GHGs) phenomenon, is regarded as one of the most serious threats humanity faces today due to its negative impact on the world [1]. CO₂ emissions are one of the most significant issues of GHGs [2]. Cement is the most common building material used as a binder (glue) in a variety of construction projects such as bridges, buildings, and roads [3, 4]. The manufacturing of one ton of cement needs about 1500 kg of raw materials and gives approximately 1000 kg of CO₂ emissions [5, 6]. The cement industry contributes 7% of all CO₂ emissions worldwide [7]. Researchers are looking for ways to bring this number down. The use of various supplemental Cementitious materials (SCMs) can be an

effective option. A difficulty SCMs are increasingly widely employed to cut costs. Through hydraulic or pozzolanic action, these compounds can increase concrete qualities like compressive strength, durability, and impermeability activity. Typically, the main component of SCM's additive is an amorphous SiO₂ that is active. Fly ash, blast furnace slag, rice husk ash, silica fume, and metakaolin are all examples of commonly used industrial by-products. Heat treatment between 600 and 800 oC of causes dehydroxylation of the crystalline structure of kaolinite, resulting in metakaolin. Kaolinitic clays are commonly available in the earth's crust [8-10].

Metakaolin (MK), Al₂Si₂O₇, MK is a newcomer to the pozzolanic materials family. It's a calcined alumino-silicate that's been thermally activated.

*Corresponding author e-mail: mohamedsultan86@Azhar.edu.eg; (Mohamed E. Sultan).

EJCHEM use only: Received date: 27 December 2022; revised date 20 February 2023; accepted date: 05 March 2023
DOI: 10.21608/EJCHEM.2023.183762.7391

©2023 National Information and Documentation Center (NIDOC)

Unlike other pozzolans, is a major product rather than a by-product or a secondary product. This enables the manufacturing process to be tailored to achieve the MK's ideal features, enabling the manufacture of a consistent product and supply. MK's white hue results in lighter-coloured concrete, which is another benefit that makes it popular [8, 11]. Is an amorphous dehydration product of Kaolinite (K) ($\text{Al}_2(\text{OH})_4\text{Si}_2\text{O}_5$) with considerable pozzolanic activity [12]. Calcination at a moderate temperature (650–800°C) is used to make MK from kaolin clay. The key to generating metakaolin for use as a supplementary cementing ingredient, or pozzolans, is to achieve complete dehydroxylation as closely as possible without overheating. Successful kaolinite processing yields a disordered amorphous state that is extremely pozzolanic [7]. The main interaction between MK and CH occurs in the presence of water and is caused by cement hydration. This reaction produces crystalline compounds such as calcium aluminate hydrate and aluminosilicate hydrates (C3AH6, C4AH13, and C2ASH8), as well as extra cementitious CSH gel. The MK/CH ratio and reaction temperature are the primary determinants of crystalline products. The binding characteristics of blended cement are improved by this process, which is even slower than the hydration of ordinary Portland cement [13]. As 30 mass percent MK is substituted for cement, the strength and transport qualities of blended concrete are significantly improved when compared to unblended concrete [13]. MK as a partial substitute for cement increased the compressive strength of concrete, however, the optimum level of OPC substitution by MK was around 20% mass percent [6, 14].

Cement kiln flue dust (CKFD) is a fine powdery particle that is produced as a waste of the cement production process. Electrostatic precipitators produce very small (micro-sized) particles, which are used to make them. During the process of making cement [15]. Kilns that are wet and dry, Cement kilns can be divided into two types: they go Slurry and dry feed materials are available. The calcium content of CKFD produced by the wet method is lower than that of CKFD produced by the dry procedure. In CKFD, the coarser particles have the largest concentration of free lime, which is collected near the kiln. Sulphates and alkalis are commonly found in high concentrations of fine particles. The chemical makeup of CKFD is similar to that of Portland

cement. Lime, iron, silica, and alumina compounds, as well as trace metals including cadmium, lead, selenium, and radionuclides, are the most common ingredients [15, 16].

Because it elevates the alkalinity of OPC, CKFD is high in alkaline oxides and chlorides, which cannot be recycled with raw material feed. Previous research has investigated the production of CKFD-OPC blends, which combine CKFD with pozzolanic materials like FA, MK, and GGBFS [17]. The work aims to study the optimum substitution ratio between OPC and MK by measuring physicochemical and mechanical properties. After selecting the best substitution ratio, incorporation of CKFD as an alkaline activator to enhance the pozzolanic activity of OPC-MK blends, especially at early ages of hydration because the previous researches evidence the OPC-MK blends exhibited low mechanical and hydration activity at early ages. The samples were analyzed by DTA, FTIR, SEM, and XRD.

2. Experimental details

2.1 Materials

The used Ordinary Portland Cement (OPC) 42.5N was supplied from Helwan Cement Company, Helwan, Egypt. The mean particle size was 13.85776μ and the D-90 was 32.7051μ as observed in Fig. 1(a). The main phases shown from XRD in Fig.2 were (C3S), (C2S), (C3A), and (C4AF). The XRF analysis in table 1. showed the presence of calcium oxide was the major component besides silica, alumina, and iron oxide. The kaolinitic clay is supplied from Sinai Manganese Company, Abu-Znima, Egypt. Metakaolin (MK) was prepared by calcining kaolin ($\text{Al}_2\text{SiO}_5 \cdot 2\text{H}_2\text{O}$) at 750 °C for 2 hours to activate it by removing structural water and converted into a disordered activated phase [18]. The particle size distribution in Fig.1(b) appears that the mean size was 19.29862μ with D-90 equals 38.3461μ . The main phases shown from XRD were quartz and mullite. The XRF analysis is in the table.1 showed the presence of silica (the major component), alumina, and iron oxide. Cement kiln flue dust (CKFD) was provided by Sinai Cement Company. The XRD spectrum of CKFD indicates the presence of many crystalline phases such as portlandite, calcite, reyerite, sylvite, and dellalite. On the other hand, the XRF analysis of CKFD evidenced the presence of the above crystal phases in XRD.

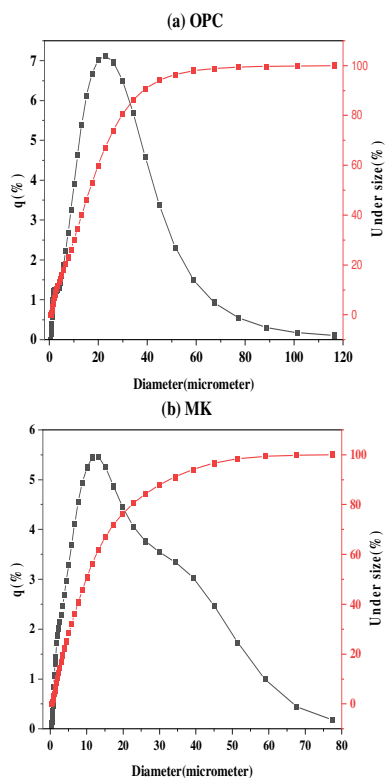


Fig. 1: Particle size distribution of (a) OPC and (b) MK

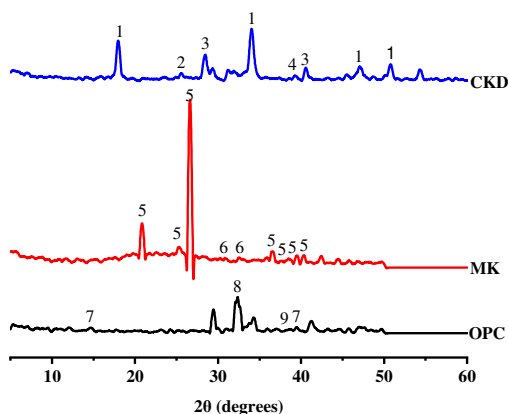


Fig. 2: XRD analysis of OPC, MK, and CKFD. (1. Portlandite, 2. Rhyerite, 3. Sylvite, 4. Dellalite, 5. Quartz, 6. Mullite, 7. β -C₂S, 8. C₃A, 9. C₃S)

2.2. Preparation of binder mixes.

Two main series were prepared as shown in Table 2. The first one was prepared from OPC with different weights of MK 5, 10, 15, 20, and 25 wt. %. To achieve the best-blended mix. Then, incorporate CKFD in the 15MK sample with different ratios of CKFD as 2, 4, 6, 8, and 10 wt. %. The dry mix was blended for 1 hour in a ball mill to form

an homogeneous mixture. Each binder mixture was sealed in a plastic bottle to keep it fresh.

Table 1

Composition of beginning materials in terms of oxides

Oxide	SampleCode			
	OPC	K	MK	CKFD
SiO ₂	21.4	54.43	62.37	10.71
Al ₂ O ₃	3.57	30.56	31.70	3.24
Fe ₂ O ₃	3.29	0.78	1.37	2.86
CaO	61.82	0.21	0.36	55.91
SO ₃	2.57	0.24	0.25	3.94
MgO	1.15	0.09	0.16	0.37
Na ₂ O	0.3	0.3	0.13	1.54
TiO ₂	---	1.65	2.60	---
P ₂ O ₅	---	0.14	0.10	---
Cl ⁻	0.09	0.11	0.03	4.661
LOI	4.53	11.40	1.16	---

Table 2

Mix design of all prepared mixes

Mix code	Material wt. %			*W/C	Setting time (min)
	OPC	MK	CKD		
OPC	100	0	0	0.254	127-221
5MK	95	5	0	0.257	86-213
10MK	90	10	0	0.263	69-198
15MK	85	15	0	0.266	60-180
20MK	80	20	0	0.272	67-185
25MK	75	25	0	0.277	78-207
0CKFD	85	15	0	0.308	69-143
2 CKFD	95	15	2	0.310	67-139
4 CKFD	90	15	4	0.313	65-136
6 CKFD	85	15	6	0.315	62-133
8 CKFD	80	15	8	0.320	60-129
10 CKFD	75	15	10	0.325	58-126

*W/C: water to cement ratio, IST:Initial setting time, FST:final setting time

To pastes preparations, the water consistency and setting times were determined by the Vicat apparatus. The water of consistency was poured into each dry mix in a hollow that was formed in the middle of a portion of the mix that was placed on a simple and non-absorbent surface. After mixing for three minutes, the paste was poured into 1-inch cube molds and vibrated to remove any air bubbles [18-20]. Directly after molding the molds were covered with plastic sheets to prevent water loss at room

temperature for 24 hours. The hardened pastes were removed from the molds and cured in tap water until the measurements were conducted at different curing ages 3, 7, 14, 28, and 56 days of hydration. The compressive strength of hardened cubes was measured at different curing ages followed by the stopping of hydration. The stopping of the hydration process was performed according to the absolute methyl alcohol and acetone method. The selected samples were grounded and powdered to measure FTIR, DTA, XRF, and XRD analysis.

2.3. Methods of investigation

Vicat apparatus was used to determine the pastes' water consistency by ASTM: C191 [21]. The compressive strength of three cubic pastes representing the same binder pastes and curing time was measured according to ASTM C-150 [18, 22], and the average result was recorded. To avoid additional hydration, the compressive strength samples were crushed and treated with a 1:1 mixture (by volume) of methyl alcohol and acetone. A porcelain mortar was used to grind dried samples weighing about 10 g, which were subsequently stored in airtight containers. Differential thermal analysis (DTA) on a dried sample in a nitrogen atmosphere (DTA-50 (Schimadzu Co. Tokyo, Japan)) was performed on a sample of roughly 15 mg with a heating rate of 20°C/min. A Bruker D8 Advanced diffractometer was used to perform X-ray diffraction (XRD) on selected hydrated binders. Cu-K α -1.54Å Germany radiation and a 25°C/min scanning speed. The morphologies of the hardened pastes were investigated using a scanning electron microscope (SEM Quanta FEG 250 with field emission gun, FEI Company - Netherlands) after a 28 days curing period [23, 24]. The chemical composition was measured by using X-Ray Fluorescence XRF (ARL 9900 Thermo Fischer).

3. Results and Discussion

3.1 Water of consistency and setting time

The water consistency and setting times of the neat OPC, OPC-MK, and OPC-MK-CKFD blended cement pastes were presented in Fig 3 and 4. The results of water consistency for MK blended cement pastes with/without CKFD were given higher values of water consumption compared with the neat OPC due to the high fineness of metakaolin and CKFD, as well as their narrow particle size distribution, the rough and porous surface for MK and CKFD. Furthermore, because MK has lower specific gravity than cement, it may have resulted in a bigger volume of paste, requiring more water to achieve the same consistency. Increasing the amount of water demand for MK and CKFD mixes is directly proportional to

the amount of MK and CKFD added [25]. The amount of MK and CKFD in a mix affects the initial and final setting times. All blended cement showed lower values for initial and final setting times than the neat OPC. The results of setting times of OPC-MK mixes showed a gradual decrease in both the initial and final setting times up to 15 MK; the increase of MK addition makes delays for the setting times due to the dilution effect and decrease of the Ca(OH)₂ which was produced from the hydration of OPC. The addition of pozzolana to OPC increases the initial setting time values compared with the final setting time [26]. The initial and final setting times for OPC-MK blended cement pastes exhibited lower values compared with the OPC paste up to 15% substitution ratio after that the setting times given gradually increased in the setting times values up to 25MK because of the increase of the substitution of OPC with MK with higher volume caused to decrease the hydration rate [26, 27]. After the addition of CKFD to 15 MK mix with different substitution values, the results of setting times exhibited lower values compared with 15MK without CKFD. The decrease of 15MK-CKFD setting times can be attributed to activation and acceleration of the outer surface of MK particles with CKFD alkalis such as sodium oxide, potassium oxide, and calcium oxide [28]. On the other hand, CKFD contains about 3.94% sulfate which increases the Ettringite formation.

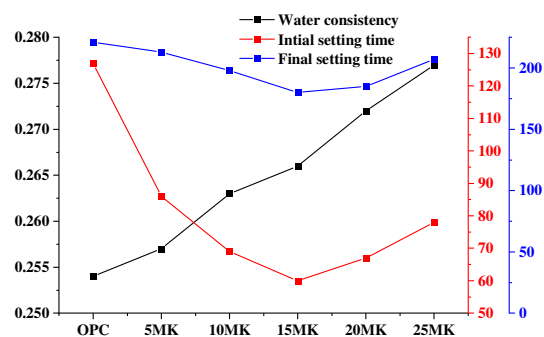


Fig. 3: Water Consistency and setting time of OPC mixes containing different ratios of MK

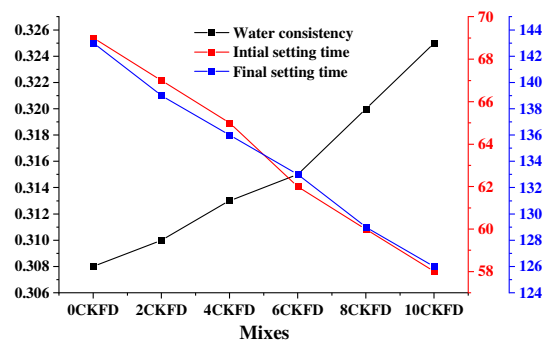


Fig. 4: Water Consistency and setting time of 15 MK mixes containing different ratios of CKFD

3.2 Compressive strength

The compressive strength of hardened OPC-MK mixes and OPC-MK-CKFDmixes after hydration for 56 days are presented in Figs. 5, 6. At the early ages of hydration, the compressive strength of OPC-MK mixes given lower values compared with the neat OPC. The compressive strength of hardened pastes composed of all mixes improves continuously with increasing age of hydration, as shown in Fig. (5) [25]. The progress of hydration products inside the pore system of hardened pastes is the main factor for this increase in the compressive strength values. Metakaolin improved cement strength significantly, especially at later ages of hydration [15, 29]. This increase can be attributed to the formation of excessive hydration products due to the pozzolanic reaction between MK and the liberated portlandite from OPC hydration [20, 30]. The pozzolanic reaction initially starts at the surface of MK particles during the formation of C-S-H and C-A-S-H Gels. The best percent of OPC-MK blended cement paste is 15MK. To accelerate the pozzolanic reaction of MK, the addition of CKFD to the OPC-MK blend improves the gel formation especially at early ages of hydration as shown in Fig. 6. This improvement was noted and extends to the later ages of hydration due to the alkaline activation of MK surface with CKFD. Incorporation of CKFD in 15MK mix exhibited the best compressive strength values up to 6%CKFD (6CKFD mix) for both early and later ages of hydration.

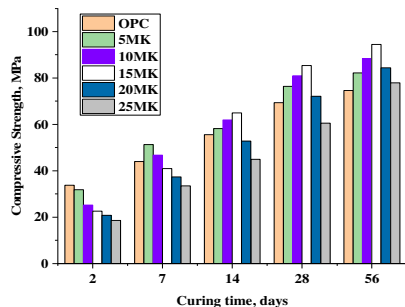


Fig. 5: Compressive Strength of the OPC and OPC- MK blends at different curing ages

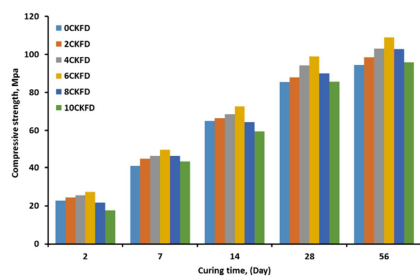


Fig. 6: Compressive Strength of the blended cement containing 15MK and different ratios of CKFD at different curing ages

3.3 FT-IR analysis

Figure 7 and 8 shows Fourier transform infrared spectroscopy (FT-IR) of hardened cement samples containing different ratios of MK measured at 7 and 28 days. The spectra clearly show a transmittance band at 3650 cm^{-1} due to the stretching vibration of the (OH) group of $\text{Ca}(\text{OH})_2$, as well as broad bands at 3450 and 1650 cm^{-1} due to $-\text{OH}$ or H_2O stretching and bending vibrations, respectively [31, 32]. The transmittance bands at 1424 , 875 , and 712 cm^{-1} are due to the presence of $(\text{CO}_3)^{-}$.

The (Si-O) transmittance bands of the C-S-H phase may account for the strong band at 970 cm^{-1} [33]. The FTIR spectra in Figure 7 after curing at 7 days show that the calcium hydroxide (CH) peaks located at 3665 cm^{-1} decrease with increasing the blending ratio with MK due to the hydration reaction and the replacing OPC with MK.

Also, there is a broad band at 3455 cm^{-1} for combined water and hydrating materials (CSH & CASH) within the sample, we observe with the addition of MK up to 25 % decrease in the band. As the results in Figure 8 after curing at 28 days show the characteristic bands of the asymmetric stretching vibration present at 980 cm^{-1} for (Si-O) are shifted approximately to a lower frequency of 970 cm^{-1} for the OPC-15MK sample at 28 days. This shift indicates the formation of amorphous aluminosilicates phases, and this is due to the effect of MK on the acceleration reaction. Also, there is a broad band at 3455 cm^{-1} for combined water and hydrating materials (CSH & CASH) within the sample, we observe with the addition of MK up to 15 % an increase in the band, and the characteristic bands of the calcium hydroxide (CH) peaks located at 3665 cm^{-1} decrease with increasing of the blending ratio with MK and this is due to the reaction of free dissolved calcium from the OPC precursor forming (CSH) which will provide additional binders.

The intensity of the band of the 15 % MK sample is higher than the other samples. On the other hand, the results indicate that when the percentage of addition is more than 15 % of MK, it leads to a decrease in the bandwidth of the blended cement at about 1050 cm^{-1} with the formation of a shoulder for solubilized silica as a result of MK agglomeration that hinders the reaction, and thus a weak region is formed in the form of voids, and thus The homogeneous hydrated microstructure could not be formed and a lower force would be possible.

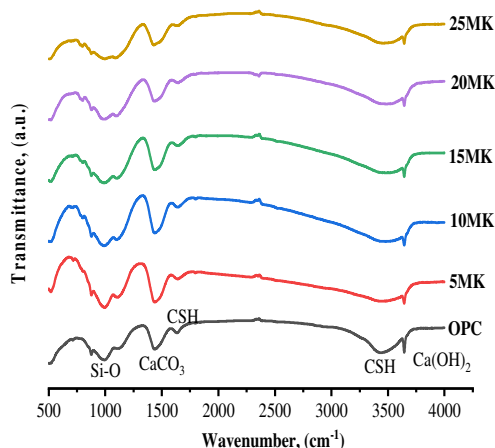


Fig. 7: The FTIR analysis of all mixes at 7 days of curing age

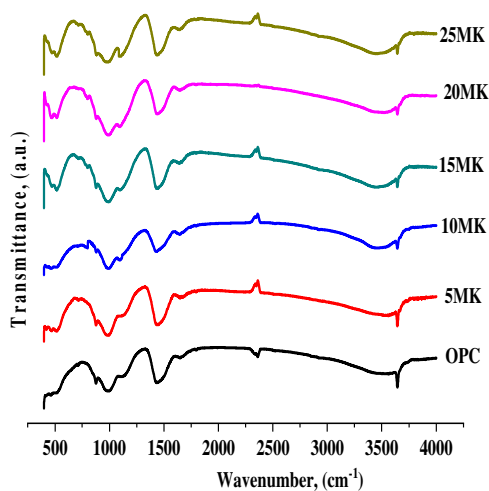


Fig. 8: The FTIR analysis of all mixes at 28 days of curing age

3.4 Differential thermal analysis (DTA)

Figures 9&10 show DTA thermograms for hardened OPC-MK mixes and OPC-MK-CKFD mixes after 28 days of hydration. The elimination of free water and the disintegration of virtually amorphous calcium silicate hydrates, primarily CSH, as well as calcium sulphoaluminate hydrates, are characterized by the first endothermic peak, which is located around 80-120°C. The

decomposition of calcium aluminate hydrates, mostly as C₄AH₁₃, as well as the crystalline CSH, is represented by the second endothermic peak, which occurs at about 140-170°C [34]. The breakdown of CH is characterized by the third endothermic peak, which is centered at about 440-470°C [35, 36]. The decomposition of amorphous CaCO₃ and its crystalline form is represented by the last endothermic peaks, which appeared at 700 to 800 °C [13]. The effect of partial replacement of OPC by MK can be observed from the thermograms shown in Figs. (9). The main features of these thermograms are the decrease in the peak area characteristic for the free Ca(OH)₂ (portlandite phase) and the increase in the peak area of CSH with an increase in MK content up to 15 % as compared to that the neat OPC paste. This is due to the formation of excessive amounts of CSH as a result of the higher pozzolanic activity of MK. Also, the intensities of the endothermic peak located at about 470-500 °C, are characteristic of the decomposition of calcium hydroxide (portlandite). The intensity of this endotherm decreases with increasing MK content up to 25 %; this is due to the dilution of cement as well as the consumption of free calcium hydroxide by the pozzolanic interaction with MK.

The effect of partial replacement of OPC-15MK with different ratios with CKFD can be observed from the thermograms shown in Figs. (10). The main features of these thermograms are the decrease in the peak area characteristic for the free Ca(OH)₂ and an increase in the peak area of CSH with an increase in CKFD containing up to 6 %. This is due to the formation of excessive amounts of CSH and Ettringite due to the positive effect of CKFD alkalis that accelerate the rate of reaction.

3.5 X-Ray Diffraction

Figs. 11, 12 shows the XRD pattern of 28 days of hardened OPC-MK mixes and OPC-MK-CKFD mixes respectively [15]. The result of Fig. 11 shows decreasing in portlandite peaks at 17, 34, and 48 degrees with increasing in MK ratios up to 15%. On another hand, increasing intensities of hydration products C-S-H and C-A-S-H with MK incorporation up to 15% due to pozzolanic reaction between amorphous alumina silicate phases with calcium hydroxide which is produced from hydration reaction [37]. The result of Fig. 12 shows the XRD analysis has been done at 28 days to evaluate the effect of CKFD addition on the OPC-15MK blend [37]. The result indicates to, the incorporation of CKFD to OPC-15MK paste with different substitution ratio improve and accelerate the pozzolanic activity of MK up to 6% CKFD, by the increase the hydration product (C-S-H, C-A-S-H) and decreasing the portlandite peaks.

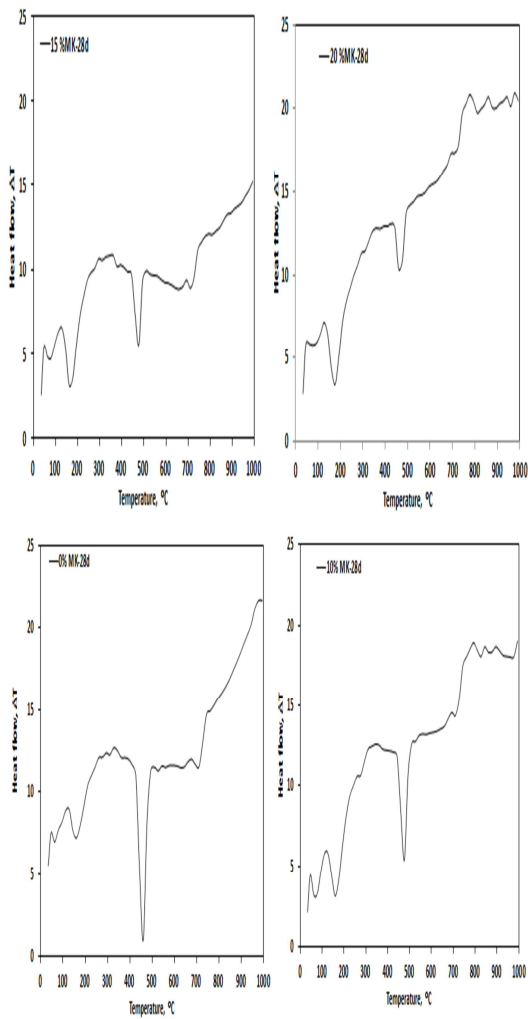


Fig. 9: The DTA analysis of 0, 10, 15, and 20 % MK mix at 28 days of hydration

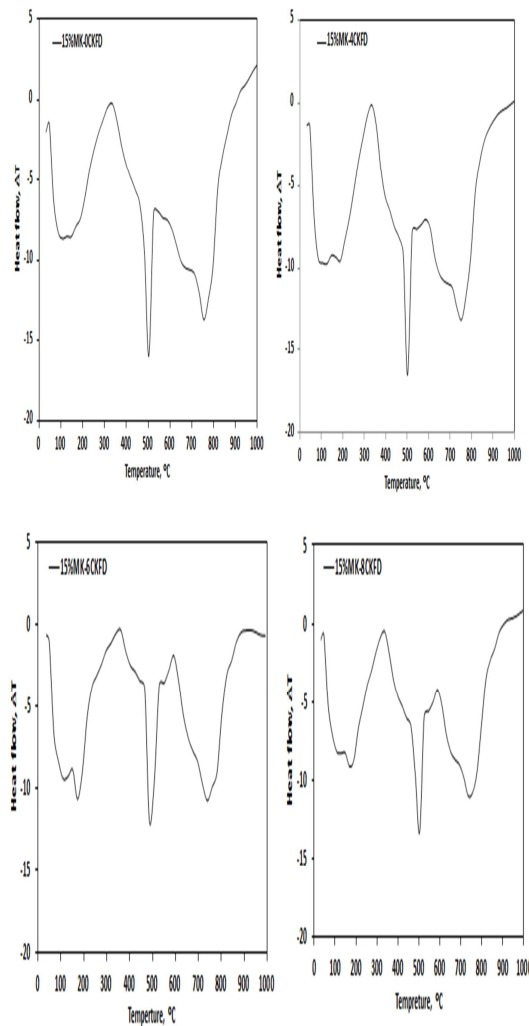


Fig10: The DTA analysis of 15 %MK containing 0, 4, 6, and 8 % CKFD mixes at 28 days of hydration

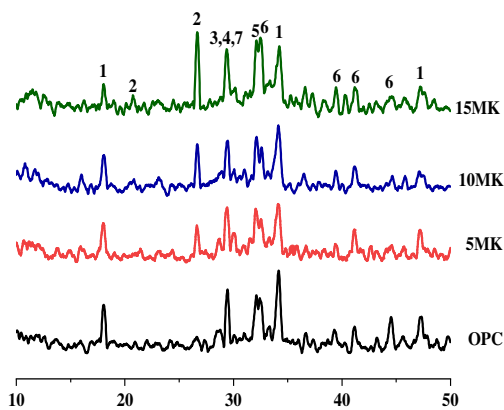


Fig11: The XRD analysis of all mixes at 28 days of curing age. (1. Portlandite 2. Quartz 3. Calcium silicate hydrates 4. Calcite 5. Alite 6. Belite 7. Calcium aluminosilicate hydrate)

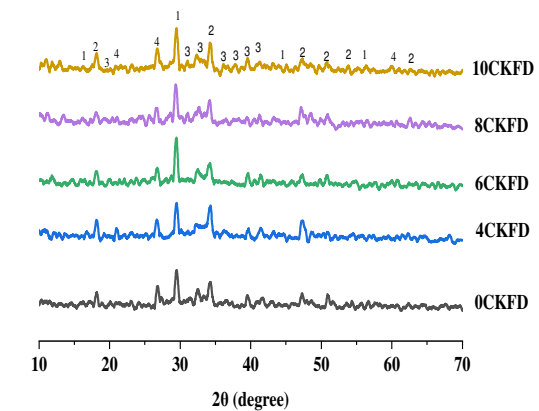


Fig. 12: The XRD analysis of all mixes at 28 days of curing age. (1. Calcium Silicate 2. Portlandite 3. Larnite 4. Quartz)

3.6 Microstructure analysis

Figure 13, and 14 shows the SEM images of OPC-MK mixes and OPC-MK-CKFD mixes after hydration for 28 days. Fig. 13 illustrates the SEM image of the neat cement sample; the micrograph shows unreacted alite and belite (C₂S, C₃S) phases, and some hydration products include hexagonal crystals of portlandite and semi-amorphous phase of CSH gel. The microstructure of this sample is dominated by some disconnected pores. With the incorporation of 15% MK, the denser microstructure can be noted due to the development of calcium silicate hydrate (Gel) from the reaction of amorphous silica with Ca (OH)₂ in OPC as well as the filler effect of the fine MK particles. These increase the packing density and compacted structure [24]. The incorporation of 25% MK leads to the formation of micropores spread throughout the matrix, which could be attributed to the dilution of cement, hence increasing the total porosity. Fig. 14 illustrates the SEM image of mixes after adding CKFD to the 15MK mix with different percentages as mentioned above the analysis improve that the ideal percentage was 6CKFD/15MK due to the presence of hydration product CSH and the absence of Ca(OH)₂ this is with previous and compressive strength [38, 39].

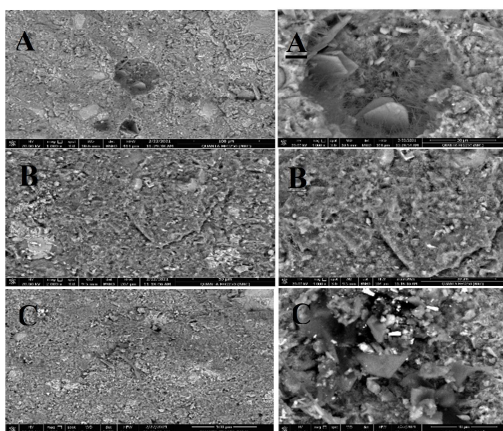


Fig.13: SEM of OPC (A, A) and MK; 10 % (B, B) and 25% (C, C) blends after 28 days of curing

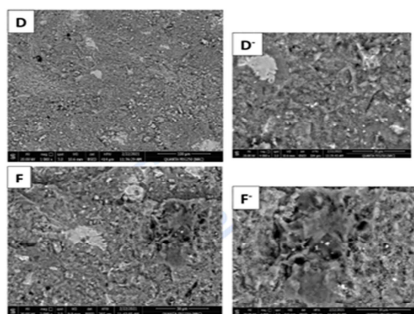


Fig. 14: SEM of 15MK blend and CKFD; 6 % (D, D') and 10% (E, E') blends after 28 days of curing

4. Conclusion

In this work, the physicochemical and blended cement mixes containing various ratios of metakaolin and cement kiln flue dust were reviewed. The most important conclusions are as follows.

- 1- The MK has a positive effect on the physicochemical of blended cement.
- 2- The 15MK mix exhibited the best results regarding the physicochemical of hardened cement paste, especially at later ages of hydration by the reaction of Ca (OH)₂ and formation of CSH which contribute to increasing the strength of mixes.
- 3- The compressive strength of the 15MK mix increased by about 23.53% compared with the neat OPC at 28 days of hydration.
- 4- Based on the physicochemical and mechanical measurement, the incorporation of 6% CKFD with 15 % MK in blended cement paste improved the physicochemical properties of the hardened cement by increasing the strength in the early ages of hydration, reducing Ca (OH)₂ and increasing CSH. Reduces waste and environmental hazards.

5. Conflicts of interest

The authors declare that there is no conflict of interest regarding the publication of this paper.

6. Acknowledgments

Many thanks to Prof. Dr. Ahmed Shabanah Professor at Al-Azhar University, Faculty of Science, Chemistry Department, Cairo, Egypt for his assistance in the revision work and valuable participation.

7. References

1. Mehta, A., & Ashish, D. K. Silica fume and waste glass in cement concrete production: A review. *Journal of Building Engineering*, 29, 100888. (2020).
2. Specht, E., Redemann, T., & Lorenz, N. Simplified mathematical model for calculating global warming through anthropogenic CO₂. *International Journal of Thermal Sciences*, 102, 1-8. (2016).
3. Karim, M. R., Zain, M. F. M., Jamil, M., & Lai, F. C. Fabrication of a non-cement binder using slag, palm oil fuel ash and rice husk ash with sodium hydroxide. *Construction and Building Materials*, 49, 894-902. (2013).
4. Saedi, M., Behfarnia, K., & Soltanian, H. The effect of the blaine fineness on the mechanical

- properties of the alkali-activated slag cement. *Journal of Building Engineering*, 26, 100897.(2019).
5. Smith, H., Joseph, A. A., Hashim, R. K., & Hashim, K. S. The Success of the Construction Industry's Adoption of the Carbon Assessment Strategy PAS2050. In *IOP Conference Series: Earth and Environmental Science* (Vol. 877, No. 1, p. 012019). IOP Publishing.(2021, November).
 6. Younes, M. M., Abdel-Rahman, H. A., & Khattab, M. M. Utilization of rice husk ash and waste glass in the production of ternary blended cement mortar composites. *Journal of Building Engineering*, 20, 42-50.(2018).
 7. Siddique, R., & Khan, M. I. Supplementary cementing materials. Springer Science & Business Media.(2011).
 8. Abdelmelek, N., & Lublóy, É. E. Improved fire resistance by using different dosages of metakaolin.(2017).
 9. Gharieb, M., Mosleh, Y. A., & Rashad, A. M. Properties and corrosion behaviour of applicable binary and ternary geopolymer blends. *International Journal of Sustainable Engineering*, 14(5), 1068-1080.(2021).
 10. Ouda, A. S., & Gharieb, M. Behavior of alkali-activated pozzocrete-fly ash paste modified with ceramic tile waste against elevated temperatures and seawater attacks. *Construction and Building Materials*, 285, 122866. (2021).
 11. Mlinárik, L., & Kopeckó, K. Impact of metakaolin-a new supplementary material-on the hydration mechanism of cements. *Acta Tech. Napocensis Civ. Eng. Archit*, 56(2), 100-110.(2013).
 12. Fernandez, R., Martirena, F., & Scrivener, K. L. The origin of the pozzolanic activity of calcined clay minerals: A comparison between kaolinite, illite and montmorillonite. *Cement and concrete research*, 41(1), 113-122.(2011).
 13. Amer, A. A., & El-Hoseny, S. Properties and performance of metakaolin pozzolanic cement pastes. *Journal of Thermal Analysis and Calorimetry*, 129(1), 33-44.(2017).
 14. Shatat, M. R., Ali, G. A., & Gouda, G. A. Effect of hydrothermal curing on hydration characteristics of metakaolin-CKD pastes at different temperatures in a closed system. *Beni-Suef University journal of basic and applied sciences*, 5(4), 299-305.(2016).
 15. Oriola, F. O. P., Moses, G., & Afolayan, J. O. Effects of combining metakaolin and cement kiln dust as cement replacement material in concrete. *Academy Journal of Science and Engineering*, 9(1), 101-111.(2015).
 16. Marku, J., Dumi, I., Lico, E., Dilo, T., & Cakaj, O. The characterization and the utilization of cement kiln dust (CKD) as partial replacement of Portland cement in mortar and concrete production. *Zaštítamaterijala*, 53, 334-344.(2012).
 17. Shatat, M. R. Effect of hydrothermal curing on the hydration characteristics of artificial pozzolanic cement pastes placed in closed system. *Applied clay science*, 96, 110-115.(2014).
 18. Abo-El-Enein, S. A., Hammad, H. M., EL-Sokary, T. M., Mekky, S. D., & Mustafa, M. E. Physico-chemical and mechanical properties of blended cement pastes containing rice husk ash and metakaolin. *Al-Azhar Bulletin of Science*, 25(1-A), 7-14.(2014).
 19. Gharieb, M., & Rashad, A. M. Impact of Sugar Beet Waste on Strength and Durability of Alkali-Activated Slag Cement. *ACI Materials Journal*, 119(2).(2022).
 20. ASTM, C. Standard test methods for time of setting of hydraulic cement by Vicat needle. C191-08.(2008).
 21. Santos, T. A., de Oliveira e Silva, G. A., & Ribeiro, D. V. Mineralogical Analysis of Portland Cement Pastes Rehydrated. *The Journal of Solid Waste Technology and Management*, 46(1), 15-23.(2020).
 22. Sultan, M. E., Abo-El-Enein, S. A., Sayed, A. Z., EL-Sokary, T. M., & Hammad, H. A. Incorporation of cement bypass flue dust in fly ash and blast furnace slag-based geopolymer. Case studies in construction materials, 8, 315-322.(2018).
 23. El-Diadamony, H., Amer, A. A., Sokkary, T. M., & El-Hoseny, S. Hydration and characteristics of metakaolin pozzolanic cement pastes. *HBRC journal*, 14(2), 150-158.(2018).
 24. Rashad, A. M., & Gharieb, M. Valorization of sugar beet waste as an additive for fly ash geopolymer cement cured at room temperature. *Journal of Building Engineering*, 44, 102989.(2021).
 25. Cho, W. J., Kim, M. J., & Kim, J. S. Study on the pore structure characteristics of ferronickel-slag-mixed ternary-blended cement. *Materials*, 13(21), 4863.(2020).
 26. Kizilkanat, A. B., Oktay, D., Kabay, N., & Tufekci, M. M. Comparative experimental study of mortars incorporating pumice powder or fly ash. *Journal of Materials in Civil Engineering*, 28(2), 04015119.(2016).
 27. Ibrahim, S. S., Hagrass, A. A., Boulos, T. R., Youssef, S. I., El-Hossiny, F. I., & Moharam, M. R. Metakaolin as an active pozzolan for cement

- that improves its properties and reduces its pollution hazard. *Journal of Minerals and Materials Characterization and Engineering*, 6(1), 86-104.(2017).
28. Hagrass, A. A., Ibrahim, S. S., El-Hosiny, F. I., Youssef, S. I., & Moharam, M. R. Hydration Characteristics of Blended Cement Containing Metakaolin. *The Bulletin Tabbin Institute for Metallurgical Studies (TIMS)*, 107(1), 38-51.(2018).
29. Mitrovic, A., & Nikolic, D. Properties of Portland-Composite Cements with metakaolin: Commercial and manufactured by Thermal Activation of Serbian Kaolin Clay. In *MATEC Web of Conferences* (Vol. 2, p. 01002). EDP Sciences.(2012).
30. Wilińska, I., Pacewska, B., & Antonovič, V. Hydration Processes of Four-Component Binders Containing a Low Amount of Cement. *Materials*, 15(6), 2192.(2022).
31. Ahmed, D. A., Mohamed, M. R., & Ebrahim, A. M. Effects of Nanometakaolin on the Physico-Chemical Characteristics of Various Blended Cement Pastes. *Journal of Scientific Research in Science*, 32(part 1), 339-354.(2015).
32. Elimbi, A., Tchakoute, H. K., Kondoh, M., & Manga, J. D. Thermal behavior and characteristics of fired geopolymers produced from local Cameroonian metakaolin. *Ceramics International*, 40(3), 4515-4520.(2014).
33. hater, H. M., & Ghareib, M. Utilization of alkaline Aluminosilicate activation in heavy metals immobilization and producing dense hybrid composites. *Arabian Journal for Science and Engineering*, 46(7), 6333-6348.(2021).
34. Rashad, A. M., & Gharieb, M. An investigation on the effect of sea sand on the properties of fly ash geopolymer mortars. *Innovative Infrastructure Solutions*, 6(2), 1-9.(2021).
35. Ahmed, D. A., Mohamed, M. R., & Ebrahim, A. M. Effects of Nanometakaolin on the Physico-Chemical Characteristics of Various Blended Cement Pastes. *Journal of Scientific Research in Science*, 32(part 1), 339-354.(2015).
36. Khalil, K. A., & Abd-El-Hameed, N. M. Physicochemical characteristics of slag rich cement pastes incorporated bypass cement dust. *Egyptian Journal of Chemistry*, 59, 491-507.(2016).
37. Zhu, X., Li, W., Du, Z., Zhou, S., Zhang, Y., & Li, F. Recycling and utilization assessment of steel slag in metakaolin based geopolymer from steel slag by-product to green geopolymer. *Construction and Building Materials*, 305, 124654.(2021).
38. Pillay, D. L., Olalusi, O. B., Kiliswa, M. W., Awoyera, P. O., Kolawole, J. T., & Babafemi, A. J. Engineering performance of metakaolin based concrete. *Cleaner Engineering and Technology*, 6, 100383.(2022).
39. Ekpo, D. U., Fajobi, A. B., Ayodele, A. L., & Etim, R. K. Potentials of cement kiln dust-periwinkle shell ash blends on plasticity properties of two selected tropical soils for use as sustainable construction materials. In *IOP Conference Series: Materials Science and Engineering* (Vol. 1036, No. 1, p. 012033). IOP Publishing.(2021, March)